Simulation of Fluid Flow in a Tesla Valve.

Hatef Khadivinassab, Daniele Rizzi

July 2, 2020

1 Introduction

Microfluidics are widely employed in areas from biomedical and drug delivery to space and fuel cell systems. Miniaturized valves (microvalves) are microfluidic two-port components that regulates the flow between two fluidic ports. These valves are the key components in devices used in drug delivery, cardiology and handling biomolecules [1] [2]. In such applications, the ability to control and move the fluid together with the ability to predict the behavior of the flow inside the valves is of utmost importance.

Microvalves come in two major categories; active and passive. Active valves use moving parts such as mechanical moving membranes that are coupled by magnetic, electric, piezoelectric or thermal actuation methods [1]. Passive valves, on the other hand, do not incorporate any moving parts, where their operational state (open or closed) is directly determined by the fluid.

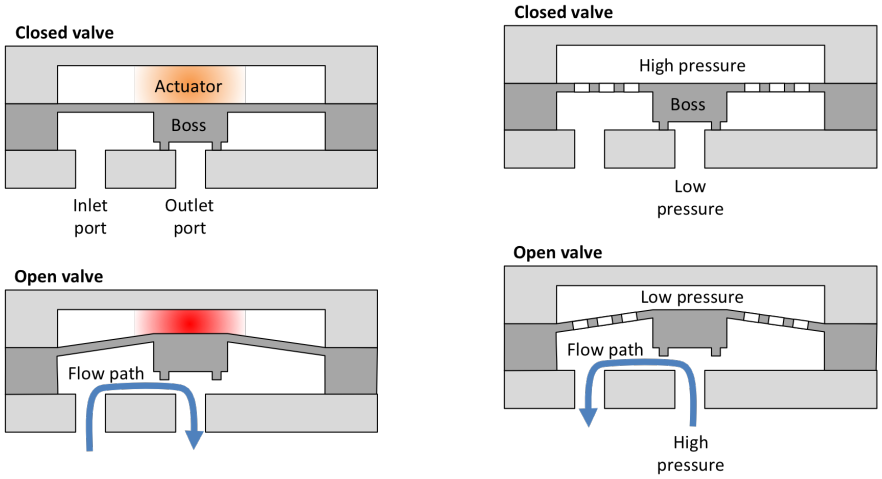

Figure 1: *Functional scheme of active (a) and passive (b) valves* [1].

Microvalves are low cost, easy to fabricate and scalable. These characteristics contribute to their increasing usage in the aforementioned industries. Despite all these advantages, their

[1]Source: `https://en.wikipedia.org/wiki/Microvalve`

operation is characterized by the equations of moving fluids in the form of the Navier-Stokes equations, whose solution is still an open problem in the field of mathematics. To predict the behavior of a moving fluid, a Computational Fluid Dynamics (CFD) simulation must be performed.

1.1 Tesla valve

Nikola Tesla patented one of the first passive valve designs. The so called Tesla valve allows flow preferentially in one direction, while prevents the flow in the other direction. The basic design of this valve consists of channel that is split in a Y junction that re-enters in a T channel, shown in Figure 2. This valve can be advantageous since it is easy to design, easy to fabricate and it can be scaled with ease.

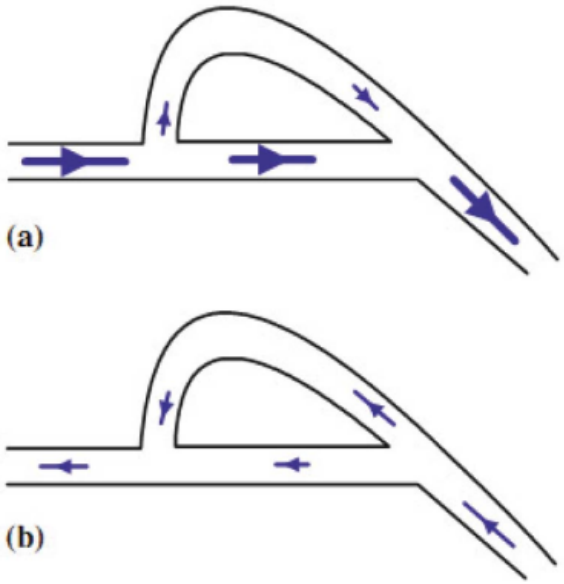

Figure 2: *Flow in a Tesla valve in forward (a) and reverse (b) direction [3].*

Such a valve, is structured to have a higher pressure drop for the flow in one direction (reverse) than the other (forward). This difference in flow resistance causes a net directional flow rate in the forward direction in oscillating flows. The efficiency is expressed in terms of the diodicity D_i, defined as the ratio of pressure drops for identical flow rates

$$D_i = \left(\frac{\Delta p_r}{\Delta p_f} \right)_Q \tag{1}$$

where Δp_r is the reverse flow pressure drop and Δp_f the forward flow pressure drop for flow rate. Since the diodicity of such valve depends on the pressure drop between direct flow versus the reverse flow, higher diodicity values may be obtained by changing geometrical parameters of this type of valve, such as:

- Angle between channel and T junction

- Angle between channel and Y junction
- Number of branches of the valve

In this paper we will analyse and discuss the diodicity of two Tesla microvalve designs with a 3D CFD simulation using the open source computing platform FEniCS.

2 Methodology

2.1 Geometry

2.1.1 Design

The Tesla valves were designed following the instructions provided in [9]. The design variables are shown in Figure 3.

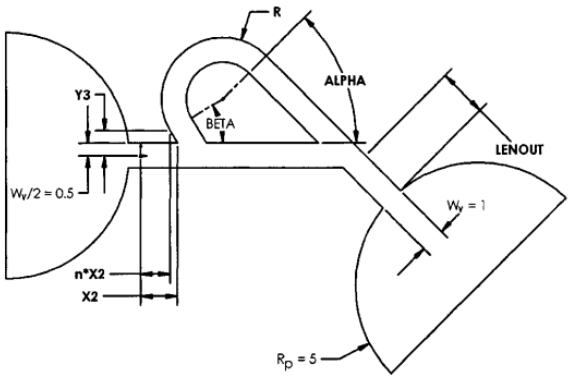

Figure 3: *Design of Tesla valve provided in [9].*

Respective dimensions for designs A (Figure 4(a)) and B (Figure 4(b)) are summarized in table 1. Note that the cross-section was assumed to be circular.

Table 1: *Dimension for different Tesla valve designs*

name	$W_y^{[mm]}$	n	$Y3^{[mm]}$	$X2^{[mm]}$	$R^{[mm]}$	$BETA^{[\circ]}$	$ALPHA^{[\circ]}$	$LENOUT^{[mm]}$
Design A	1	0.990	0.600	1.5	2.50	8.53	45.0	2.00
Design B	1	0.797	0.608	1.6	2.35	71.1	41.9	2.94

2.1.2 Mesh

The meshed geometries for design A and design B are shown in Figures 5(a) amd 5(b), respectively. The mesh statistics are shown in table 2.

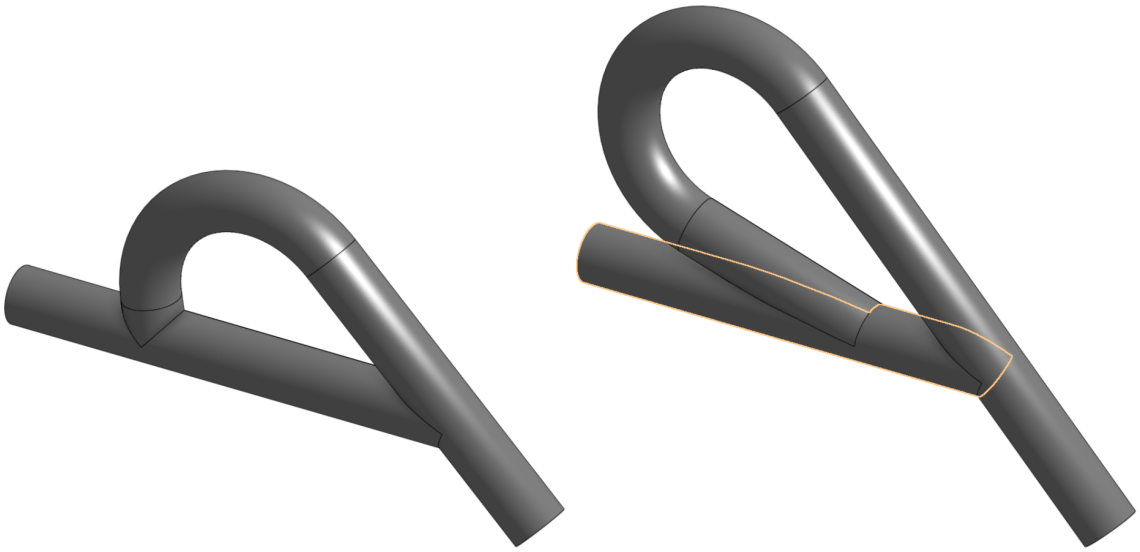

(a) (b)

Figure 4: *Tesla valve design A (a) and design B (b) used for this simulation.*

(a) (b)

Figure 5: *Tesla valve mesh for design A (a) and design B (b) used for this simulation.*

Table 2: *Mesh statistics for designs A and B.*

name	Nodes	Triangles	Tetrahedra
Design A	11680	11576	51832
Design B	12445	12552	54848

2.2 Numerical Model

2.2.1 Flow Equations

The flow equations are the Navier Stokes equations for incompressible flow, which in the strong form can be stated as:

$$\dot{u} + \nabla u \cdot u - \nu \Delta u + \nabla p = f \quad (2)$$
$$\nabla \cdot u = 0 \quad (3)$$

where u is the unknown velocity, p is the pressure field, ν is the given kinematic viscosity and f a given source. The Navier Stokes equations can be rewritten in the finite element weak form as:

$$F = \left(\frac{u - u_0}{dt}, v \right) + (\nabla u_m \cdot u_m, v) + \nu \left(\nabla u_m, \nabla v \right) + (\nabla p, v) + (\nabla \cdot u_m, q) - (f, v) \quad (4)$$

where $u_m = \theta u + (1 - \theta) u_0$ with $\theta = 0.5$ in the Crank-Nicholson scheme.

2.2.2 Stabilization methods

It is well known that the numerical solution of Navier-Stokes equations using Finite Element Methods suffers from two sources of numerical instabilities [4] [5]:

- Using wrong combination of velocity and pressure finite element spaces (that do not satisfy the inf-sup condition) generate numerical oscillations in the pressure field (spurious pressure).
- When the problem is convection-dominated ($Re >> 1$), numerical oscllations in the velocity field occurs (called spurious velocity).

These sources of instabilities may be controlled in two ways:

- Using appropriate combination of velocity and pressure finite element spaces.
- Adding stabilization terms to the weak formulation of the problem.

The first item can be addressed by using a 'P_k - P_{k+1}' combination of spaces for the unknown velocity and pressure fields. Such mixed formulation is expressed in FEniCS with the following lines of code, in which the Vector Element space $Q_e = P_1$ for the pressure and the space $V_e = P_2$ for the velocity and mixed in the space $W = V_e \times Q_e = P_k \times P_{k+1} = P_1 \times P_2$.

```
Ve = VectorElement("CG", mesh.ufl_cell(), 2)
Qe = FiniteElement("CG", mesh.ufl_cell(), 1)
W = FunctionSpace(mesh, Ve * Qe)

# Define test functions
w = Function(W)
u, p = split(w)
(v, q) = TestFunctions(W)
w0 = Function(W)
u0, _ = split(w0)
```

The second way to reduce numerical instabilities is to add to the weak formulation a stabilization term as expressed in [4], [5] and [6]. In our formulation the stabilization term is the following

$$F_{stabilization} = \tau \left[(\nabla p + \nabla u_m \cdot u_m - f, \nabla q + \nabla v \cdot u_m) + (\nabla \cdot u_m, \nabla \cdot v) \right] \tag{5}$$

where $\tau = h$ is the stabilization parameter, with h the mean mesh cell diameter.

2.2.3 Boundary Condition

The inlet velocity is assumed to have velocity only along the x-axis with a paraboloid profile with the following shape:

$$v_{in} = U(1 - \frac{y^2}{R^2} - \frac{z^2}{R^2}) \tag{6}$$

where R is the radius of the conduct and U is the maximum value of the velocity profile. Velocity components along y and z are supposed to have zero values. Dirichlet no-slip condition is applied on the walls of the valve and the outlet is assumed to discharge to atmospheric pressure.

2.2.4 Numerical Analysis

In order to characterize the diodicity of the tesla valves, three flow cases with different inlet velocities are considered. The velocity profile for these cases are as shown on Eq 6 Three maximum velocities are, $0.3m/s$, $1.5m/s$ and $5m/s$. Simulations are run until steady state is reached. Diodicity is then calculated using Eq 1.

The material used in the simulation is water with density of $1000kg/m^3$ and dynamic viscosity of $0.001Pa.s$. The code does not have any understanding of the geometrical scale, thus it assumes m units. In order to scale down the geometry to mm level we instead scaled down the density by a factor of 1000. Utilizing this method we ensure that the Reynolds number stays the same.

3 Software Workflow

The CAD geometry is designed using OnShape[2]. An exported 3D *.step* file is imported into GmSH[3] to define the mesh and surface boundaries. The mesh is then exported as a *.msh* file and is converted to *.xdmf* domain and boundary files using meshio library[4]. The calculations are performed using FEniCS open source computing platform. ParaView[5] is used for the visualization and post-processing of the results.

[2] `https://www.onshape.com/`
[3] `https://gmsh.info/`
[4] `https://github.com/nschloe/meshio`
[5] `https://www.paraview.org/`

4 Results and discussion

Each simulation, ran on 5 parallel threads, took on average 1 hour to calculate up to 30 seconds of in-simulation time using an Intel i7-7820HK (8) @ 3.900GHz CPU.

The velocity profiles at steady state are shown in figures 7 to 12. Diodicity values for each case is tabulated in table 3.

As it can be seen by comparing the velocity profiles of forward (figures on the left) and reverse flow (figures on the right), in all the simulated cases velocity fields of forward and reverse flow are significantly different.
In the forward flow simulations (figures on the left), the fluid inside the Tesla microvalve is accelerated from the inlet to the outlet. Some of the fluid goes into the side channel when reaching the T-junction which contributes to a reduction in the diodicity.
On the other hand, in the reverse flow simulations (figures on the right) the fluid is again accelerated at the inlet but it is splitted in the main and side channel when reaching the Y junction. The main and side flows then continue until they reach the T-junction, when the side flow is re-injected in the main channel. This stage is very important in the evaluation of the diodicity of the valve; when the side flow is injected in the main one, it contributes to obstacle the main flow and generates an increase in the pressure drop between the inlet and the outlet of the valve. Due to the definition of the diodicity as the ratio between the pressure drop of the reverse flow over the pressure drop of the forward flow, when the reverse pressure drop increases, the diodicity increases too.

4.1 Diodicity versus inlet velocity

The effect of the inlet velocity on the diodicity is visible in table 3. As it can be seen by comparing the results at the three different inlet velocities taken into account in the simulation, the diodicity of the same Tesla valve increases with the inlet velocity.
This effect can be explained by comparing the different behavior of the reverse flow at different inlet velocities. In the case of reverse flow, the flow is splitted in the side and main channel when reaching the Y-junction. At inlet velocity $0.3m/s$, we can see the the flow is splitted equally in the side and main channel. When the inlet velocity increases ($1.5m/s$ and $5.0m/s$), an higher volume of fluid is drained into the side channel with respect to the main channel; in this condition, when the side flow is re-injected in the main channel, it opposes to the main flow with the effect of increasing the pressure drop. By definition of the diodicity 1, the increase in the reverse pressure drop causes an increase in the diodicity.

4.2 Diodicity versus valve geometry

The geometry of the Tesla microvalve has an important effect on the diodicity too. In this project we simulated the different flow of a Tesla microvalve in which the angle BETA (defined in figure 3) has been increased from the value 8.53 of Design A to 71.1 of Design B. As one can imagine, when the angle of the T-junction is increased, the side flow is expected to be more opposed to the main flow causing higher reverse pressure drops in Design B with respect to Design A. However, as reported in table 3, we found that the diodicity values of Design A and B are the same in the case of inlet velocity $0.3m/s$, and at inlet velocities

$1.5m/s$ and $5.0m/s$ they are even lower in the case of Design B with respect to Design A. This unexpected result could be explained by the presence of flaws in the model implemented in the simulation, which does not take into account capillarity, a physical effect important when studying the behavior of fluids in micro channels, or flaws in the design that should be studied deeper by evaluating the diodicity in other Tesla valve designs.

Table 3: *Diodicity values for designs A and B at different inlet velocities.*

name	$U = 0.3m/s$	$U = 1.5m/s$	$U = 5m/s$
Design A	1.0061	1.2807	1.3796
Design B	1.0079	1.1429	1.3440

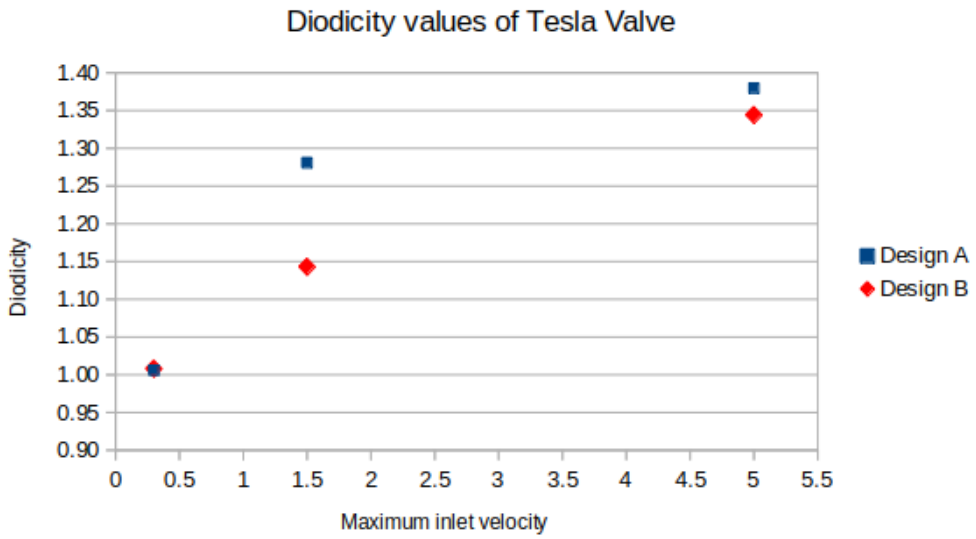

Figure 6: *Diodicity values of Design A and Design B Tesla microvalves at different inlet velocities.*

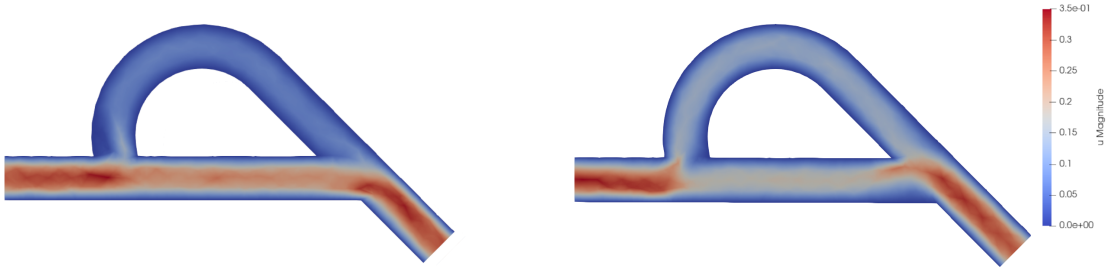

(a) (b)

Figure 7: *Velocity results for design A with $U = 0.3m/s$ with forward flow (a) and reverse flow (b).*

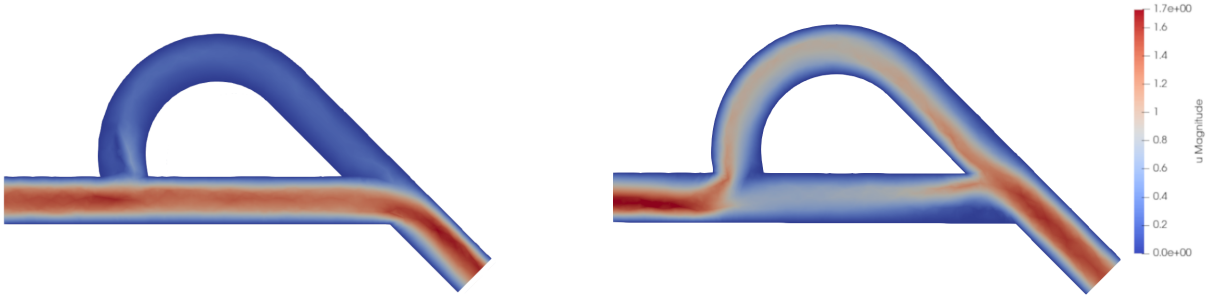

(a) (b)

Figure 8: *Velocity results for design A with $U = 1.5m/s$ with forward flow (a) and reverse flow (b).*

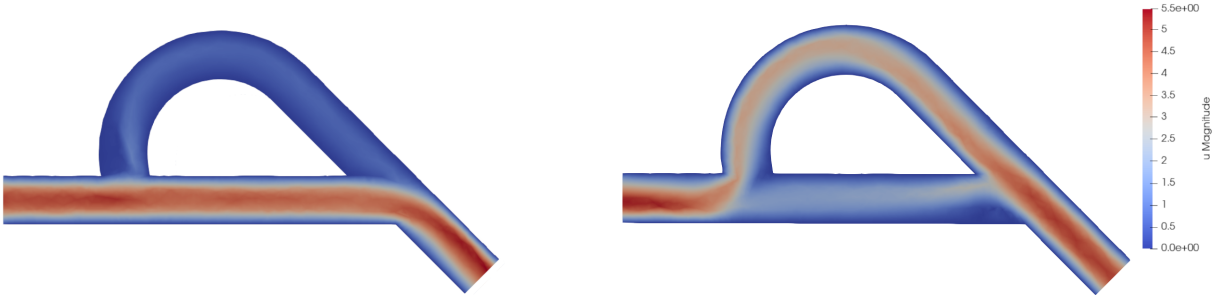

(a) (b)

Figure 9: *Velocity results for design A with $U = 5m/s$ with forward flow (a) and reverse flow (b).*

(a) (b)

Figure 10: *Velocity results for design B with $U = 0.3m/s$ with forward flow (a) and reverse flow (b).*

(a) (b)

Figure 11: *Velocity results for design B with $U = 1.5m/s$ with forward flow (a) and reverse flow (b).*

(a) (b)

Figure 12: *Velocity results for design B with $U = 5m/s$ with forward flow (a) and reverse flow (b).*

5 Conclusions and Future Work

In our work we simulated the behavior of flow in a Tesla microvalve. We then evaluated the impact of the inlet velocity and of the different Tesla valve design on the diodicity.
As a result we found that the diodicity of the Tesla valve increases with the inlet velocity. On the contrary, we found that the effect of the different Tesla valve geometry results in unexpected diodicity values.

We believe a comprehensive sensitivity analysis on Tesla Valve design would be beneficial to understand how these parameters affect the diodicity. Moreover, at micro scales capillary forces become very important in characterizing the flow. We would like to investigate the effects of such forces.

It would also be interesting to utilize Fenics' automated mesh refinement on this case to reduce simulation time.

References

[1] Kwang, Chong,*A review of microvalves*, J. Micromech. Microeng. 16 (2006)

[2] Jin-Yuan Qian, Cong-Wei Hou, Xiao-Juan Li and Zhi-Jiang Jin, *Actuation Mechanism of Microvalves: A Review*, Micromachines 2020, 11, 172

[3] A. Y. Nobakht, M. Shahsavan, A. Paykani, *Numerical Study of Diodicity Mechanism in Different Tesla-Type Microvalves*, Journal of Applied Research and Technology, Vol.11, December 2013

[4] T.E. Tezduyar, *Stabilized finite element formulations for incompressible flow computations*, Advances in Applied Mechanics, 28 (1992) 1-44

[5] T.E. Tezduyar, S. Mittal, S.E. Ray and R. Shih, *Incompressible flow computations with stabilized bilinear and linear equal-order-interpolation velocity-pressure elements*, Computer Methods in Applied Mechanics and Engineering, 95 (1992) 221-242

[6] J. Jansson, E. Krishnasamy, M. Leoni, N. Jansson and J. Hoffman, *Time-resolved Adaptive Direct FEM Simulation of High-lift Aircraft Configurations*

[7] A. Logg, H. P. Langtangen, *Solving PDEs in Python*, Springer 2017

[8] A. Logg, K. A. Mardal, G. N. Wells, *Automated Solution of Differential Equations by the Finite Element Method*, Springer 2017

[9] A. Gamboa, C. Morris, F. Foster, *Improvements in Fixed-Valve Micropump Performance Through Shape Optimization of Valves*, Journal of Fluids Engineering, March 2005, Vol. 127